



Universiteit  
Leiden  
The Netherlands

## Structural and functional models for [NiFe] hydrogenase

Angamuthu, R.

### Citation

Angamuthu, R. (2009, October 14). *Structural and functional models for [NiFe] hydrogenase*. Retrieved from <https://hdl.handle.net/1887/14052>

Version: Corrected Publisher's Version

License: [Licence agreement concerning inclusion of doctoral thesis in the Institutional Repository of the University of Leiden](#)

Downloaded from: <https://hdl.handle.net/1887/14052>

**Note:** To cite this publication please use the final published version (if applicable).

# Synthesis, Characterization and Electrocatalytic Properties of $[\text{Ni}(\text{S}_4)\text{Fe}(\text{C}_5\text{H}_5)(\text{CO})](\text{PF}_6)$ Complexes Containing Bidentate $\text{SS}'$ -donor Ligands<sup>†</sup>

**Abstract.** Five bidentate chelating  $\text{SS}'$ -donor ligands – abbreviated as Hbsms, Hmpsms, Hcpsms, Hibsms and Hnhsms – have been synthesized that differ in electronic properties. These ligands have been reacted with  $[\text{Ni}(\text{acac})_2]$  (acac = acetylacetonate) and the low-spin nickel complexes of general formula  $[\text{Ni}(\text{SS}')_2]$  have been obtained. Reaction of these low-spin nickel complexes with  $[\text{Fe}(\text{C}_5\text{H}_5)(\text{CO})_2]$  ( $\text{C}_5\text{H}_5$  = cyclopentadienyl) and anion exchange with  $\text{NH}_4\text{PF}_6$  yielded five new  $[\text{NiFe}]$  complexes of general formula  $[\text{Ni}(\text{SS}')_2\text{Fe}(\text{C}_5\text{H}_5)(\text{CO})](\text{PF}_6)$ . All the nickel and  $[\text{NiFe}]$  complexes have been characterized using ESI-MS spectrometry, electronic absorption and IR spectroscopy, and cyclic voltammetric techniques. The X-ray structure of the nickel complex with the ligand Hcpsms is reported; the compound crystallizes as the trimer  $[\text{Ni}_3(\text{cpsms})_6]$  with two different  $\text{NiS}_4$  coordination environments as four of the six ligands bind as monodentate and the remaining two bind as chelating bidentate ligands. Three of the five  $[\text{NiFe}]$  complexes show electrocatalytic activity to produce dihydrogen in the presence of acetic acid. Catalytic reduction of  $\text{H}^+$  is found to occur at potentials as low as  $-0.9$  V vs.  $\text{Ag}/\text{AgCl}$  for  $[\text{Ni}(\text{mpsms})_2\text{Fe}(\text{C}_5\text{H}_5)(\text{CO})](\text{PF}_6)$ ,  $[\text{Ni}(\text{ibsms})_2\text{Fe}(\text{C}_5\text{H}_5)(\text{CO})](\text{PF}_6)$  and  $[\text{Ni}(\text{nhsms})_2\text{Fe}(\text{C}_5\text{H}_5)(\text{CO})](\text{PF}_6)$  in acetonitrile. It is thus concluded that increased flexibility in the  $\text{S}_4$  coordination sphere of the nickel(II) ion favors the lower overpotentials. The thioether donors of the chelating bidentate ligands are more readily protonated than in the chelating tetradentate ligands reported in Chapter 3; this leads to the rapid decomposition of the complexes  $[\text{Ni}(\text{bsms})_2\text{Fe}(\text{C}_5\text{H}_5)(\text{CO})](\text{PF}_6)$  and  $[\text{Ni}(\text{cpsms})_2\text{Fe}(\text{C}_5\text{H}_5)(\text{CO})](\text{PF}_6)$ .

---

<sup>†</sup> This chapter is based on: R. Angamuthu, M. A. Siegler, A. L. Spek and E. Bouwman, *manuscript in preparation*.

## 4.1. Introduction

The [NiFe] complexes of  $S_2S'_2$ -donor tetradentate ligands reported in Chapter 3 are electrocatalytically reducing protons at potentials in the range of  $-1.74$  to  $-1.19$  V vs. Ag/AgCl. It was found that the potential at which proton reduction occurs is shifted positively upon increasing the flexibility of the ligands. Furthermore, the [NiFe] complexes  $[Ni(bsms)_2Fe(CO)_2I_2]$  ( $E_{pc} = -0.8$  V vs. Ag/AgCl),  $[Ni(bss)_2Fe(CO)_2I_2]$  ( $E_{pc} = -0.92$  V vs. Ag/AgCl) and  $[Ni(bsms)_2FeI_2]_2$  ( $E_{pc} = -0.79$  V vs. Ag/AgCl) containing bidentate ligands (Fig. 4.2), synthesized by Bouwman and coworkers exhibit less negative reduction potentials compared to the [NiFe] complexes reported in Chapter 3.<sup>1</sup> Hence, the bidentate  $SS'$ -donor ligands, of which the synthesis is described in Chapter 2, have been used in the synthesis of [NiFe] complexes in order to evaluate the effect of the increased flexibility in these new complexes on their proton reduction capability.

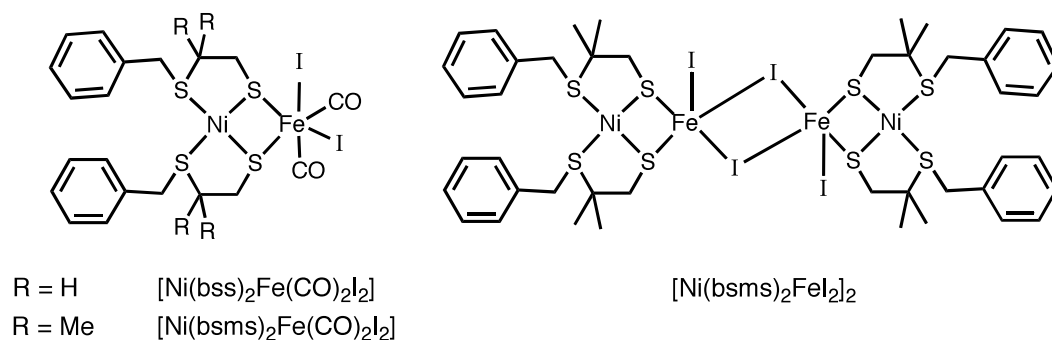


Fig. 4.1. Schematic representations of the complexes synthesized by Bouwman and coworkers.<sup>1</sup>

A number of nickel complexes are known to have bidentate  $S_2$ - and  $PS$ -donor ligands<sup>1-15</sup>, these ligands mostly tend to produce either tetrahedral  $[Ni(SS)_2]$ -mononuclear, or oligonuclear complexes. This Chapter deals with the syntheses and characterizations of four new  $[Ni(SS')_2]$  complexes of the bidentate  $SS'$ -donor ligands Hmpsms, Hcpsms, Hibsms and Hnhmsms (Fig. 4.2). Also, the syntheses, characterizations and electrocatalytic properties of five new complexes of general formula  $[Ni(SS')_2Fe(C_5H_5)(CO)](PF_6)$  are discussed.

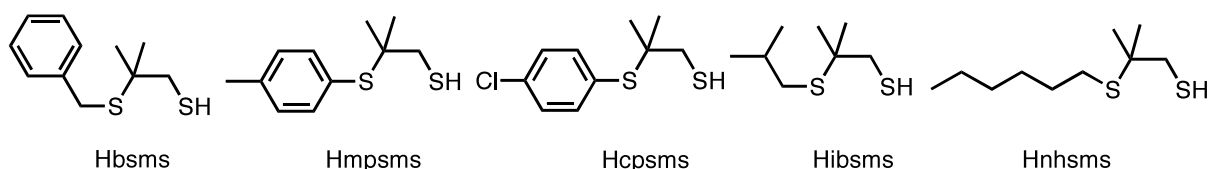


Fig. 4.2. Bidentate chelating ligands used in the present study (see Chapter-2, section 2.2 for the abbreviation of the names of ligands).

## 4.2. Results

### 4.2.1. Synthesis

The syntheses of ligand precursor thiuronium salts are discussed in detail in Chapter 2. The low-spin square-planar  $[\text{Ni}(\text{SS}')_2]$  complexes are synthesized by the reaction of  $\text{Ni}(\text{acac})_2$  with two equivalents of the thiuronium chloride salt of the ligands, in the presence of two equivalents of tetramethylammonium hydroxide. Even though these complexes could be synthesized in protic solvents, such as ethanol in relatively high yields, using toluene as the solvent leads to further improvement. The complexes  $[\text{Ni}(\text{bsms})_2]$  (shiny brick-red crystalline)<sup>12</sup> and  $[\text{Ni}(\text{mpsms})_2]$  (dark brown microcrystalline) are very stable as solid and in solution under air, whereas the complexes  $[\text{Ni}(\text{cpsms})_2]$ ,  $[\text{Ni}(\text{ibsms})_2]$ , and  $[\text{Ni}(\text{nhsms})_2]$  are slightly hygroscopic in air, but stable in an argon atmosphere for months. The syntheses of nickel(II) complexes of the unsubstituted ligands Hcpss and Hmpss yielded the hexanuclear  $[\text{Ni}_6(\text{cpss})_{12}]$  metallacrown and an insoluble brick-red precipitate, respectively. The synthesis, structure and electrocatalytic properties of the hexanuclear complex  $[\text{Ni}_6(\text{cpss})_{12}]$  has been studied in detail and will be reported in Chapter 6.

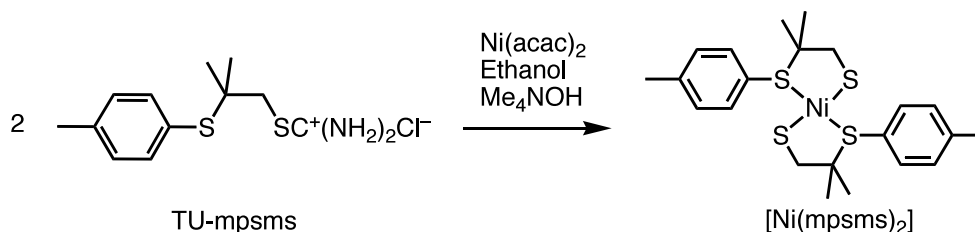


Fig. 4.3. Illustrative synthetic route used in the synthesis of  $[\text{Ni}(\text{SS}')_2]$  complexes.

The  $[\text{NiFe}]$  complexes were synthesized following the same procedure as reported in Chapter 3 for the tetradentate ligands. All five nickel complexes reported in this chapter have been reacted with  $[\text{Fe}(\text{C}_5\text{H}_5)(\text{CO})_2\text{I}]$  for 12 hours in order to form  $[\text{NiFe}]$  complexes of general formula  $[\text{Ni}(\text{SS}')_2\text{Fe}(\text{C}_5\text{H}_5)(\text{CO})]\text{I}$ . Performing this initial step of the reaction in a closed argon atmosphere gives rise to a mixture of complexes analyzed as  $[\text{Ni}(\text{SS}')_2\text{Fe}(\text{C}_5\text{H}_5)(\text{CO})]^+$  and  $[\text{Ni}(\text{SS}')_2\text{Fe}(\text{C}_5\text{H}_5)(\text{CO})_2]^+$ , as observed from the ESI-MS spectra, and eventually this mixture decomposes in air. To avoid the formation of this mixture, argon was purged into the solution throughout the reaction time and the evaporated dichloromethane was regularly replaced; this yielded relatively pure monocarbonyl derivatives, which are stable enough to be manipulated in air for weighing and transferring. The iodide anions are exchanged with  $\text{PF}_6^-$  anions using an exact stoichiometric amount of  $\text{NH}_4\text{PF}_6$ . The formed ammonium iodide and any unwanted

precipitates are removed by passing the solution through a Celite column. The analytically pure [NiFe] complexes are obtained as their PF<sub>6</sub> salts, by passing the acetonitrile solutions of the complexes through a neutral alumina column.

#### 4.2.2. Molecular Structure of the [Ni(SS')<sub>2</sub>] Complexes

The molecular structure of the complex [Ni(bsms)<sub>2</sub>] has been reported by Bouwman and coworkers.<sup>12</sup> Single crystals suitable for X-ray diffraction were obtained for [Ni(mpsms)<sub>2</sub>]<sub>3</sub>. The complex [Ni(cpsms)<sub>2</sub>]<sub>3</sub> crystallizes in the space group C2/c; the asymmetric unit contains one crystallographically independent ordered molecule and a molecule of dichloromethane. Even though the complex of nickel(II) with the ligand Hcpsms is observed to be monomeric in solution, the X-ray crystal determination revealed a linear trinuclear [Ni<sub>3</sub>(cpsms)<sub>6</sub>] molecule, containing three square-planar NiS<sub>4</sub> units joined by edge sharing, in which only two of the ligands are chelating and the remaining four are coordinating as monodentate via the thiolate sulfur (Fig. 4.4). The observed structural reorganization may be caused by the protic solvent (ethanol) used in the crystallization process. The coordination environments of the two terminal NiS<sub>4</sub> units differ from the central NiS<sub>4</sub> unit. The terminal nickel(II) centers (Ni2, Ni3) are coordinated by a chelating ligand and two μ-S thiolate donors of two monodentate ligands, whereas the central nickel(II) ion Ni1 is coordinated to four μ-S thiolate donors.

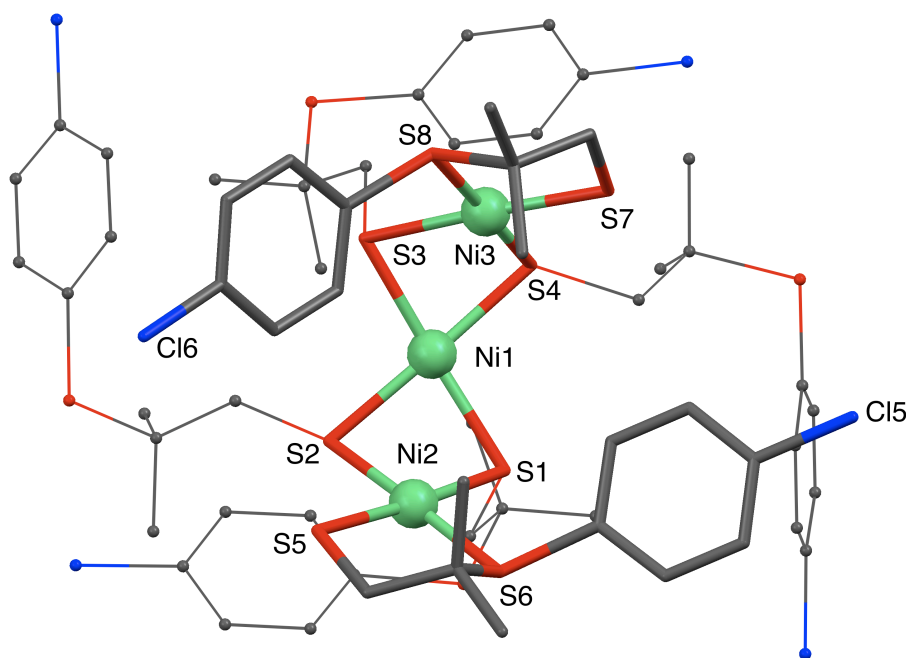


Fig. 4.4. Perspective view of [Ni<sub>3</sub>(cpsms)<sub>6</sub>]. Ni, green; S, red, C, gray, Cl, blue. Chelating ligands shown in capped stick model, monodentate ligands shown in minimized ball and stick model for the sake of clarity. Dichloromethane and hydrogen atoms have been omitted for clarity. Ni1···Ni2, 2.9104(6) Å; Ni1···Ni3, 2.8774(7) Å; Ni2···Ni3, 4.8856(7) Å. Further details are provided in Table 4.1

The two Ni–S<sub>thiolate</sub> distances (2.1655(11), 2.1670(12) Å) of the chelating ligands are shorter than (or equal to) the two Ni–S<sub>thioether</sub> distances (2.1647(10), 2.1700(11) Å), as expected. These two Ni–S<sub>thiolate</sub> distances are shorter than those of the bridging monodentate ligands (2.1751(9)–2.2388(9) Å). Owing to the geometrical restrictions introduced by the thiolate and thioether donors, the NiS<sub>4</sub> units are not strictly planar; the nickel ions Ni1, Ni2 and Ni3 are 0.069, 0.035 and 0.030 Å above their corresponding S<sub>4</sub> planes, respectively. The central NiS<sub>4</sub> basal plane has a considerably high degree of tetrahedral distortion with a dihedral angle of 13.74° (between the planes S1–Ni1–S2 and S3–Ni1–S4), whereas smaller dihedral angles of 3.68° for Ni2 (between the planes S1–Ni2–S2 and S5–Ni2–S6) and 3.07° for Ni3 (between the planes S3–Ni3–S4 and S7–Ni3–S8) are observed. The S–Ni–S *cis* bond angles range from 80.31(4) to 100.07(4).

The X-ray crystal structure of [Ni(bsms)<sub>2</sub>] has been reported in literature and revealed a perfectly planar mononuclear structure – due to the inversion center at the nickel ion – comprising the two thiolate donors and two thioether donors coordinated to the nickel(II) center in *trans* positions.<sup>12</sup> The X-ray crystal structure of a derivative of the complex [Ni(mpsms)<sub>2</sub>] has been reported recently and is discussed in detail in Chapter 7. This compound contains two [Ni(mpsms)<sub>2</sub>] units bridged together *via* six CuI units in which each [Ni(mpsms)<sub>2</sub>] unit has two thiolate donors and two thioether donors coordinated to the nickel(II) center in enforced *cis* positions.<sup>16</sup>

Table 4.1. Selected distances (Å) and angles (°) for [Ni<sub>3</sub>(cpsms)<sub>6</sub>].

Ni1–S1	2.2233(10)	Ni2–S1	2.2388(9)	Ni3–S3	2.2353(11)
Ni1–S2	2.1897(10)	Ni2–S2	2.1827(10)	Ni3–S4	2.1751(9)
Ni1–S3	2.2269(11)	Ni2–S5	2.1655(11)	Ni3–S7	2.1670(12)
Ni1–S4	2.1931(10)	Ni2–S6	2.1647(10)	Ni3–S8	2.1700(11)
S1–Ni1–S2	81.51(4)	S1–Ni2–S2	81.31(3)	S3–Ni3–S4	80.76(4)
S1–Ni1–S3	168.05(4)	S1–Ni2–S5	175.09(4)	S3–Ni3–S7	174.96(4)
S1–Ni1–S4	100.07(4)	S1–Ni2–S6	96.15(4)	S3–Ni3–S8	95.75(4)
S2–Ni1–S3	98.89(4)	S2–Ni2–S5	93.78(4)	S4–Ni3–S7	94.20(4)
S2–Ni1–S4	175.04(4)	S2–Ni2–S6	175.53(4)	S4–Ni3–S8	175.36(4)
S3–Ni1–S4	80.56(4)	S5–Ni2–S6	88.76(4)	S7–Ni3–S8	89.28(4)
Ni1–S1–Ni2	81.42(3)	Ni1–S2–Ni2	83.46(4)		
Ni1–S3–Ni3	80.31(4)	Ni1–S4–Ni3	82.40(3)		

### 4.2.3. Electronic, NMR and ESI-MS Spectra of the Nickel Complexes

The electronic spectra of the nickel(II) complexes have been recorded in chloroform solutions (Table 4.2). All the five nickel complexes exhibit two characteristic bands between 14000 cm<sup>-1</sup> (<sup>1</sup>E' ← <sup>1</sup>A<sub>1</sub>') and 24000 cm<sup>-1</sup> (<sup>1</sup>E'' ← <sup>1</sup>A<sub>1</sub>') due to d←d transitions, consistent with the square-planar geometry expected for an NiS<sub>4</sub> chromophore. The absorption maxima of these complexes are at slightly higher energies

compared to those of the  $[\text{Ni}(\text{S}_2\text{S}'_2)]$  complexes reported in Chapter 3; this may be caused by the *trans* location of the thiolates and the freedom of having perfect square-planarity, as observed in the X-ray crystal structure of  $[\text{Ni}(\text{bsms})_2]$ .<sup>12</sup> Furthermore, the bands observed around 19000 and 24000  $\text{cm}^{-1}$  for the  $[\text{Ni}(\text{S}_2\text{S}'_2)]$  complexes are located around 21000 and 28000  $\text{cm}^{-1}$ , respectively, for the nickel complexes of the bidentate ligands. The absorption maxima of  $[\text{Ni}(\text{cpsms})_2]$  are shifted to slightly lower energy than those of  $[\text{Ni}(\text{mpsms})_2]$  due to the electron-withdrawing *p*-chlorophenyl ring in  $[\text{Ni}(\text{cpsms})_2]$ .

Table 4.2. Electronic absorption maxima for the nickel complexes measured in chloroform and the *m/z* values of the parent molecular ion peaks observed in ESI-MS.

Complex	$\nu/10^3 \text{ cm}^{-1}$ ( $\epsilon/\text{mol}^{-1} \text{ l cm}^{-1}$ )					<i>m/z</i> of $[\text{M}+\text{H}^+]$ exptl. (calcd.)
$[\text{Ni}(\text{bsms})_2]$	14.4 (96)	22.0 (360)	28.2 (6600)	33.6 (12900)	38.1 (15000)	480.78 (481.07)
$[\text{Ni}(\text{mpsms})_2]$	14.8 (47)	21.4 (230)	29.4 (6500)	33.9 (11600)	36.6 (13800)	480.80 (481.07)
$[\text{Ni}(\text{cpsms})_2]$	14.8 (39)	20.1 (281)	28.6 (1514)	33.6 (5300)	37.5 (6900)	520.75 (520.96)
$[\text{Ni}(\text{ibsms})_2]$	14.5 (25)	21.1 (121)	28.6 (3900)	33.0 (5800)	35.6 (6500)	39.1 (6700) 412.93 (413.10)
$[\text{Ni}(\text{nhsms})_2]$	14.8 (46)	20.3 (570)	28.6 (4500)	33.0 (5900)	35.6 (6800)	39.1 (7760) 468.98 (469.16)

The room temperature  $^1\text{H}$  NMR spectra of the complexes  $[\text{Ni}(\text{mpsms})_2]$ ,  $[\text{Ni}(\text{cpsms})_2]$  and  $[\text{Ni}(\text{nhsms})_2]$  show relatively sharp signals compared to the complexes  $[\text{Ni}(\text{ibsms})_2]$  and  $[\text{Ni}(\text{bsms})_2]$ . This is probably due to the interesting fact that the *ortho*-protons of the 4-methylphenyl and 4-chlorophenyl rings of the complexes  $[\text{Ni}(\text{mpsms})_2]$  and  $[\text{Ni}(\text{cpsms})_2]$ , respectively, interact with the axial positions of the nickel(II) ion. This is evident from the broad signal observed at around 8 ppm in the  $^1\text{H}$  NMR spectra of the complexes  $[\text{Ni}(\text{mpsms})_2]$  and  $[\text{Ni}(\text{cpsms})_2]$  at 303 K. This interesting phenomenon is also observed in the derived cluster compound  $\{[\text{Ni}(\text{mpsms})_2]\text{(CuI)}_6\}$ , both in the solid-state structure ( $\text{Ni}\cdots\text{H} = 2.626$  to  $2.781 \text{ \AA}$ ) and in solution (7.8 ppm at 303 K, 9.5 ppm at 183 K), as studied by variable temperature  $^1\text{H}$  NMR spectroscopy. The sharp signals observed in the case of  $[\text{Ni}(\text{nhsms})_2]$  can be explained by the fact that the relatively long *n*-hexyl groups may restrict the fast *cis-trans* isomerisation. More detailed NMR studies including variable temperature and 2D NMR techniques are necessary to shed light into these interesting phenomena in solution.

ESI-MS spectra of all the complexes were obtained from dichloromethane solutions containing trace amounts of acetic acid. Despite the fact that the complex  $[\text{Ni}(\text{cpsms})_2]$  exhibits a trinuclear structure in the solid state, in all the cases the

$[\text{Ni}(\text{SS}')_2+\text{H}]^+$  molecular ion peaks were observed, perfectly matching with calculated isotopic distributions.

Table 4.3. Electrochemical data of the  $[\text{Ni}(\text{SS}')_2]$  complexes obtained for 1 mM solutions in dichloromethane containing 0.1 M  $(\text{NBu}_4)\text{PF}_6$ . Scan rate  $200 \text{ mV s}^{-1}$ . Static GC disc working electrode, Pt wire counter electrodes with a  $\text{Ag}/\text{AgCl}$  (satd. KCl) reference electrode.

Complex	$E_{\text{pa}}(\text{V})$	$E_{\text{pc}}(\text{V})$
$[\text{Ni}(\text{bsms})_2]$	0.63	
	-0.35	-0.83
$[\text{Ni}(\text{mpsms})_2]$	0.62	
	-0.31	-0.80
$[\text{Ni}(\text{cpsms})_2]$	0.73	
		-0.61
$[\text{Ni}(\text{ibsms})_2]$	0.61	
	-0.37	
	-0.50	-0.79
$[\text{Ni}(\text{nhsms})_2]$	0.58	
	-0.38	
	-0.53	
		-0.84

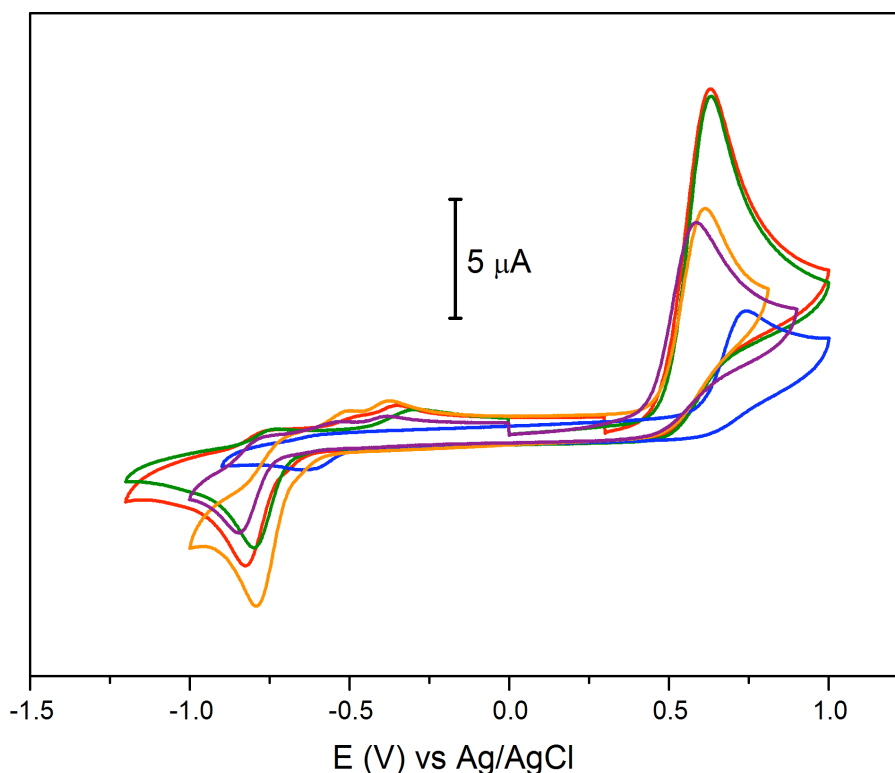


Fig. 4.5. Cyclic voltammograms of  $[\text{Ni}(\text{bsms})_2]$  (red),  $[\text{Ni}(\text{mpsms})_2]$  (green),  $[\text{Ni}(\text{cpsms})_2]$  (blue),  $[\text{Ni}(\text{ibsms})_2]$  (orange) and  $[\text{Ni}(\text{nhsms})_2]$  (purple); see Table 4.3 for more details.



#### 4.2.4. Electrochemical Behaviour of the Nickel Complexes

The electrochemical properties of the  $[\text{Ni}(\text{SS}')_2]$  complexes were investigated (Fig. 4.5) using cyclic voltammetry; the relevant data are presented in Table 4.3. At a scan rate of  $200 \text{ mV s}^{-1}$  only irreversible oxidations of the complexes are observed at potentials ranging between 0.58 and 0.73 V vs. Ag/AgCl (Table 4.5), which are comparable to the  $[\text{Ni}(\text{S}_2\text{S}'_2)]$  complexes reported in Chapter 3. The oxidation potential of  $[\text{Ni}(\text{cpsms})_2]$  is 0.11 V higher than that of  $[\text{Ni}(\text{mpsms})_2]$  due to the electron-withdrawing *p*-chlorophenyl ring in  $[\text{Ni}(\text{cpsms})_2]$ . This trend is also reflected in the reduction potentials of the complexes  $[\text{Ni}(\text{mpsms})_2]$  and  $[\text{Ni}(\text{cpsms})_2]$ ; the complex  $[\text{Ni}(\text{cpsms})_2]$  ( $-0.61 \text{ V vs. Ag/AgCl}$ ) is more readily reduced than the complex  $[\text{Ni}(\text{mpsms})_2]$  ( $-0.80 \text{ V vs. Ag/AgCl}$ ).

#### 4.2.5. ESI-MS, FTIR and Electronic Spectra of the [NiFe] Complexes

The characterization of the  $[\text{NiFe}]$  complexes using ESI-MS spectrometry was performed using freshly prepared acetonitrile solutions. In all the cases molecular ion and fragmentation peaks in agreement with the formulations  $[\text{Ni}(\text{SS}')_2\text{Fe}(\text{C}_5\text{H}_5)(\text{CO})]^+$ ,  $[\text{Ni}(\text{SS}')_2\text{Fe}(\text{C}_5\text{H}_5)]^+$  and  $[\text{Ni}(\text{SS}')_2\text{Fe}]^+$  were observed. The calculated and observed *m/z* values of the fragment  $[\text{Ni}(\text{SS}')_2\text{Fe}(\text{C}_5\text{H}_5)(\text{CO})]^+$  are provided in Table 4.4 along with the observed carbonyl stretching frequencies.

The carbonyl stretching frequencies of the  $[\text{NiFe}]$  complexes appear at slightly higher energies than that of the  $[\text{NiFe}]$  complexes of the tetradentate  $\text{S}_2\text{S}'_2$ -donor ligands reported in Chapter 3, suggesting that iron(II) ions possess relatively less electron density in  $[\text{Ni}(\text{SS}')_2\text{Fe}(\text{C}_5\text{H}_5)(\text{CO})](\text{PF}_6)$  complexes. This is probably due to the global electron-withdrawing effect of the aromatic groups attached to the thioether sulfurs.

The  $^1\text{H}$  NMR spectra of the  $[\text{Ni}(\text{SS}')_2\text{Fe}(\text{C}_5\text{H}_5)(\text{CO})](\text{PF}_6)$  complexes in dichloromethane exhibit broad signals, similar to the  $[\text{Ni}(\text{S}_2\text{S}'_2)\text{Fe}(\text{C}_5\text{H}_5)(\text{CO})](\text{PF}_6)$  complexes. Hence, the NMR spectroscopic data of the  $[\text{NiFe}]$  complexes are not helpful in the description of the solution structures and are not further discussed.

The UV-VIS spectra of the  $[\text{NiFe}]$  complexes have been recorded in acetonitrile and the relevant data are reported in Table 4.5. The  $d \leftarrow d$  bands of the  $\text{NiS}_4$  moiety shift to lower energy in the  $[\text{Ni}(\text{SS}')_2\text{Fe}(\text{C}_5\text{H}_5)(\text{CO})](\text{PF}_6)$  complexes compared to the corresponding mononuclear nickel complexes, which is in contrast to the  $[\text{Ni}(\text{S}_2\text{S}'_2)\text{Fe}(\text{C}_5\text{H}_5)(\text{CO})](\text{PF}_6)$  complexes. A number of higher energy bands corresponding to  $\pi \rightarrow \pi^*$  transitions of the  $\text{Cp}^-$  ring are observed between  $28000 \text{ cm}^{-1}$  and  $44000 \text{ cm}^{-1}$ .

Table 4.4. Comparison of the carbonyl IR stretching frequencies of the [NiFe] complexes in dichloromethane and the observed  $m/z$  values of the parent molecular ion peaks  $[\text{Ni}(\text{SS}')_2\text{Fe}(\text{C}_5\text{H}_5)(\text{CO})]^+$  in ESI-MS.

Complex	$\nu(\text{CO})$			$\nu(\text{PF}_6^-)$	$m/z$
					exptl. (calcd.)
$[\text{Ni}(\text{bsms})_2\text{Fe}(\text{C}_5\text{H}_5)(\text{CO})(\text{PF}_6)]$	2051,	2042,	1998	847	628.72 (629.03)
$[\text{Ni}(\text{mpsms})_2\text{Fe}(\text{C}_5\text{H}_5)(\text{CO})(\text{PF}_6)]$	2055,	2046,	2001	847	628.76 (629.03)
$[\text{Ni}(\text{cpsms})_2\text{Fe}(\text{C}_5\text{H}_5)(\text{CO})(\text{PF}_6)]$	2055,	2042,	1998	848	668.60 (668.92)
$[\text{Ni}(\text{ibsms})_2\text{Fe}(\text{C}_5\text{H}_5)(\text{CO})(\text{PF}_6)]$	2042,		1998	846	560.79 (561.06)
$[\text{Ni}(\text{nhsms})_2\text{Fe}(\text{C}_5\text{H}_5)(\text{CO})(\text{PF}_6)]$	2042,		1998	848	616.94 (617.12)

Table 4.5. Electronic absorption maxima for the  $[\text{Ni}(\text{SS}')_2\text{Fe}(\text{C}_5\text{H}_5)(\text{CO})(\text{PF}_6)]$  complexes in acetonitrile solutions.

Complex	$\nu/10^3 \text{ cm}^{-1}$ ( $\epsilon/\text{mol}^{-1} \text{ l cm}^{-1}$ )					
	$[\text{Ni}(\text{bsms})_2\text{Fe}(\text{C}_5\text{H}_5)(\text{CO})(\text{PF}_6)]$	13.6 (91)	19.6 (sh)	26.0 (3100)	33.2 (9000)	37.9 (sh)
$[\text{Ni}(\text{mpsms})_2\text{Fe}(\text{C}_5\text{H}_5)(\text{CO})(\text{PF}_6)]$	14.8 (106)	19.8 (sh)	26.0 (sh)	33.4 (11.6)	38.8 (sh)	44.4 (40.4)
$[\text{Ni}(\text{cpsms})_2\text{Fe}(\text{C}_5\text{H}_5)(\text{CO})(\text{PF}_6)]$	14.8 (39)	19.6 (281)		33.6 (5300)	38.8 (6900)	44.4 (30.3)
$[\text{Ni}(\text{ibsms})_2\text{Fe}(\text{C}_5\text{H}_5)(\text{CO})(\text{PF}_6)]$	13.6 (88)	19.6 (sh)	25.6 (sh)	33.3 (9000)	41.2 (13800)	44.6 (sh)
$[\text{Ni}(\text{nhsms})_2\text{Fe}(\text{C}_5\text{H}_5)(\text{CO})(\text{PF}_6)]$	13.6 (116)	19.5 (sh)	25.9 (4600)	33.6 (12700)	38.0 (13700)	39.1 (sh)

#### 4.2.6. Electrochemical Behaviour of the [NiFe] Complexes and Reduction of Protons

The electrochemical behavior of the [NiFe] complexes in acetonitrile was investigated using cyclic voltammetry. For all the five [NiFe] complexes several quasi-reversible and irreversible redox couples are observed (Table 4.6). As an example, the CV of the complex  $[\text{Ni}(\text{ibsms})_2\text{Fe}(\text{C}_5\text{H}_5)(\text{CO})(\text{PF}_6)]$  is shown in Fig. 4.6. In all the five [NiFe] complexes, an irreversible anodic peak is observed around 0.5 V vs Ag/AgCl corresponding to the oxidation of the nickel(II) ion to nickel(III). An irreversible reduction is observed around -1 V vs. Ag/AgCl, except for the complex  $[\text{Ni}(\text{cpsms})_2\text{Fe}(\text{C}_5\text{H}_5)(\text{CO})(\text{PF}_6)]$  which exhibits a reduction wave at -0.58 V vs. Ag/AgCl. Unfortunately, the observed oxidations and reductions cannot be unequivocally assigned, due to the presence of multiple redox-active partners in the [NiFe] complexes, and the redox changes may be distributed among the redox-active members of the [NiFe] complexes.<sup>17</sup>

Table 4.6. Electrochemical data of  $[\text{Ni}(\text{SS}')_2\text{Fe}(\text{C}_5\text{H}_5)(\text{CO})](\text{PF}_6)$  complexes (0.5 mM) in acetonitrile.\*

Complex	$E_{\text{pa}}(\text{V})$	$E_{\text{pc}}(\text{V})$	$E_{\text{HER}}(\text{V})^\#$
$[\text{Ni}(\text{bsms})_2\text{Fe}(\text{C}_5\text{H}_5)(\text{CO})](\text{PF}_6)$	0.99		
	0.50		
	0.33		
	-0.35		
		-0.93	
$[\text{Ni}(\text{mpsms})_2\text{Fe}(\text{C}_5\text{H}_5)(\text{CO})](\text{PF}_6)$	0.45		
		-0.95	-0.93
$[\text{Ni}(\text{cpsms})_2\text{Fe}(\text{C}_5\text{H}_5)(\text{CO})](\text{PF}_6)$	1.05		
	0.64		
		-0.58	
$[\text{Ni}(\text{ibsms})_2\text{Fe}(\text{C}_5\text{H}_5)(\text{CO})](\text{PF}_6)$	0.47		
		-1.04	-0.92
$[\text{Ni}(\text{nhsms})_2\text{Fe}(\text{C}_5\text{H}_5)(\text{CO})](\text{PF}_6)$	0.47		
	0.26		
		-0.64	
		-1.11	-0.94

\* Measured vs. Ag/AgCl reference electrode; Static glassy carbon disc working electrode; Pt-wire counter electrode; Scan rate 200  $\text{mV s}^{-1}$ ; Supporting electrolyte 0.05 M  $\text{Bu}_4\text{NPF}_6$ .

#  $E_{\text{HER}}$ : potential at which hydrogen evolution reaction occurs.

The electrocatalytic properties of all the five  $[\text{NiFe}]$  complexes were investigated by means of the reduction of protons using acetic acid as a relatively mild source of protons. A new irreversible cathodic wave, corresponding to the reduction of protons with concurrent evolution of dihydrogen gas, appears in the cyclic voltammograms of the  $[\text{NiFe}]$  complexes in the presence of acetic acid, which rises in height upon increasing concentrations of acetic acid (Fig. 4.6) for the complexes  $[\text{Ni}(\text{mpsms})_2\text{Fe}(\text{C}_5\text{H}_5)(\text{CO})](\text{PF}_6)$ ,  $[\text{Ni}(\text{ibsms})_2\text{Fe}(\text{C}_5\text{H}_5)(\text{CO})](\text{PF}_6)$  and  $[\text{Ni}(\text{nhsms})_2\text{Fe}(\text{C}_5\text{H}_5)(\text{CO})](\text{PF}_6)$ . The potential at which proton reduction occurs lies around  $-0.9$  V vs. Ag/AgCl. These proton reduction potentials ( $E_{\text{HER}}$ ) are less negative than those observed for the  $[\text{Ni}(\text{S}_2\text{S}'_2)\text{Fe}(\text{C}_5\text{H}_5)(\text{CO})](\text{PF}_6)$  complexes with tetradentate ligands, as was expected. Unlike the  $[\text{Ni}(\text{S}_2\text{S}'_2)\text{Fe}(\text{C}_5\text{H}_5)(\text{CO})](\text{PF}_6)$  complexes reported in Chapter 3, the electrocatalytic waves appeared slightly lower than the reduction potentials of the  $[\text{Ni}(\text{S}_2\text{S}'_2)\text{Fe}(\text{C}_5\text{H}_5)(\text{CO})](\text{PF}_6)$  complexes with a slight increase in the height of the oxidation waves. This is probably due to the protonation of the thioether sulfurs prior to the reduction making the  $[\text{Ni}(\text{S}_2\text{S}'_2)\text{Fe}(\text{C}_5\text{H}_5)(\text{CO})](\text{PF}_6)$  complexes easily reducible and more active than the  $[\text{Ni}(\text{S}_2\text{S}'_2)\text{Fe}(\text{C}_5\text{H}_5)(\text{CO})](\text{PF}_6)$  complexes.<sup>18-20</sup> This hypothesis is also supported by the observed increase in the current of the reduction wave in the range of  $-0.6$  to  $-0.8$  V vs. Ag/AgCl, before the electrocatalytic wave begins to appear (Fig. 4.6). The complexes  $[\text{Ni}(\text{bsms})_2\text{Fe}(\text{C}_5\text{H}_5)(\text{CO})](\text{PF}_6)$  and

$[\text{Ni}(\text{cpsms})_2\text{Fe}(\text{C}_5\text{H}_5)(\text{CO})](\text{PF}_6)$  are not stable in acidic solutions and eventually decompose with an accompanying change in color from brown to greenish yellow.

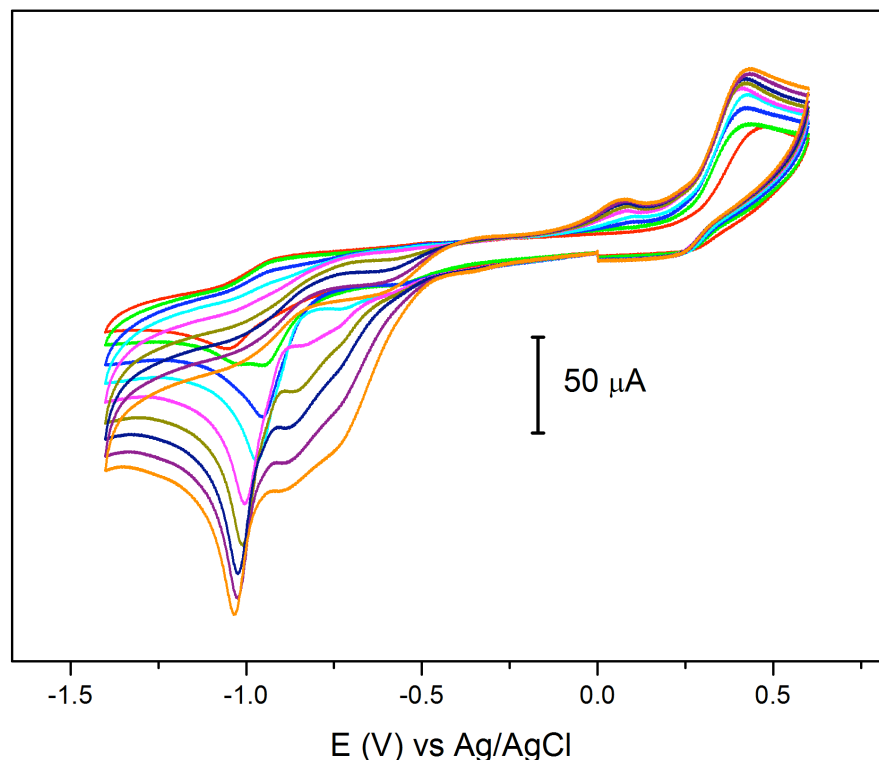


Fig. 4.6. Cyclic voltammograms of  $[\text{Ni}(\text{ibsms})_2\text{Fe}(\text{C}_5\text{H}_5)(\text{CO})](\text{PF}_6)$  (0.5 mM) in acetonitrile in the presence of 0–16 equivalents of acetic acid; additions were made with increments of 2 equivalents. Further details are provided in Table 4.6.

### 4.3. Discussion

The new nickel(II) complexes of the bidentate ligands all are mononuclear in solution, as they all exhibit the  $[\text{Ni}(\text{SS}')_2+\text{H}]^+$  peak as the parent molecular ion peak in the ESI-MS spectra. However, the complex of nickel(II) with the ligand Hcpsms crystallizes as a linear trinuclear molecule with two different  $\text{NiS}_4$  coordination environments by utilizing the ligand cpsms<sup>-</sup> not only as a monodentate, but also as a chelating bidentate ligand. This may be due to the electron-withdrawing properties of the *p*-chlorophenyl group, reducing the coordination strength of the thioether sulfur, and predominating the electron-donating ability of the dimethyl substituents. The trimerization may also be ascribed to the use of the protic solvent used in the crystallization process (ethanol/hexane). The bidentate ligand Hcps – the unsubstituted analog of the ligand Hcpsms – exhibits the same versatility in binding to the nickel(II) center as a monodentate and chelating bidentate ligand, as will be described in Chapter 6.<sup>19,21</sup> However, the nickel(II) complex of the ligand Hcps remains a hexanuclear molecule both in solid state

and in solution and the mononuclear compound  $[\text{Ni}(\text{cpss})_2]$  is not observed in ESI-MS spectrometry.

The molecular structure of the nickel(II) complex  $[\text{Ni}(\text{bsms})_2]$  is reported by Bouwman and coworkers to have a perfectly square-planar  $\text{NiS}_4$  geometry.<sup>1</sup> The complex  $[\text{Ni}(\text{mpsms})_2]$  yields a hetero-octaanuclear compound upon reacting with  $\text{CuI}$  in which the thiolate and thioether donors are bound to the nickel(II) ion in an enforced *cis* fashion on binding to the copper(I) ions (see Chapter 7). Hence, it is evident that the five  $[\text{Ni}(\text{SS}')_2]$  complexes can have either *cis* or *trans* geometry according to the situation and most probably they all remain in the highly favored *trans* forms in the mononuclear complex in solution, or in a dynamic equilibrium of these two forms. The  $[\text{NiFe}]$  complexes formed with these five  $[\text{Ni}(\text{SS}')_2]$  complexes most likely have a structure similar to that reported for the complex  $[\text{Ni}(\text{pbss})\text{Fe}(\text{C}_5\text{H}_5)(\text{CO})](\text{PF}_6)$ <sup>22</sup> with a *cis*  $\text{NiS}_4$  moiety bound to the  $[\text{Fe}(\text{C}_5\text{H}_5)(\text{CO})]^+$  group, as suggested by the available data.

The reduction potentials of the  $[\text{Ni}(\text{SS}')_2]$  complexes are found to be sensitive to the substituent groups on the thioether sulfur as observed from the cyclic voltammograms of the complexes (see section 0). Also, these reduction potentials are less negative compared to those of the  $[\text{Ni}(\text{S}_2\text{S}'_2)]$  complexes with the more rigid tetradentate ligands reported in Chapter 3.

The complexes  $[\text{Ni}(\text{bsms})_2\text{Fe}(\text{C}_5\text{H}_5)(\text{CO})](\text{PF}_6)$  and  $[\text{Ni}(\text{cpsms})_2\text{Fe}(\text{C}_5\text{H}_5)(\text{CO})](\text{PF}_6)$  are not stable in the presence of protic acids and decompose immediately upon the addition of acids. This is probably due to the fact that the thioether donors are now highly prone to undergo protonation that may lead to decomposition.<sup>19</sup> However, the complexes  $[\text{Ni}(\text{mpsms})_2\text{Fe}(\text{C}_5\text{H}_5)(\text{CO})](\text{PF}_6)$ ,  $[\text{Ni}(\text{ibsms})_2\text{Fe}(\text{C}_5\text{H}_5)(\text{CO})](\text{PF}_6)$  and  $[\text{Ni}(\text{nhsms})_2\text{Fe}(\text{C}_5\text{H}_5)(\text{CO})](\text{PF}_6)$  are found to be active electrocatalysts in the reduction of protons into dihydrogen. Interestingly, the three active  $[\text{Ni}(\text{SS}')_2\text{Fe}(\text{C}_5\text{H}_5)(\text{CO})](\text{PF}_6)$  complexes are able to reduce protons at less negative potentials, as compared to the  $[\text{Ni}(\text{S}_2\text{S}'_2)\text{Fe}(\text{C}_5\text{H}_5)(\text{CO})](\text{PF}_6)$  complexes with tetradentate ligands as expected; most likely the increased flexibility of the  $\text{NiS}_4$  coordination sphere might be responsible for this behavior. However, the  $E_{\text{HER}}$  does not seem to be affected by the electronic properties of the ligands in these complexes as they all work around  $-0.9$  V vs.  $\text{Ag}/\text{AgCl}$ ; it is possible that the flexibility of the ligands is predominant over the electronic properties of the ligands affecting the  $E_{\text{HER}}$ .

It appears – according to the available observations – that the  $[\text{Ni}(\text{S}_2\text{S}'_2)\text{Fe}(\text{C}_5\text{H}_5)(\text{CO})](\text{PF}_6)$  complexes readily undergo protonation on the thioether sulfurs of the bidentate  $\text{SS}'$ -donor ligands; this protonation is advantageous, as this behavior assists in reducing the complexes easily; on the other hand it is disadvantageous

because it leads to the decomposition of the complexes  $[\text{Ni}(\text{bsms})_2\text{Fe}(\text{C}_5\text{H}_5)(\text{CO})](\text{PF}_6)$  and  $[\text{Ni}(\text{cpsms})_2\text{Fe}(\text{C}_5\text{H}_5)(\text{CO})](\text{PF}_6)$ .

#### 4.4. Conclusions

Four new  $[\text{Ni}(\text{SS}')_2]$  complexes comprising bidentate SS'-donor ligands have been successfully synthesized. The  $^1\text{H}$  NMR spectra of the complexes  $[\text{Ni}(\text{mpsms})_2]$  and  $[\text{Ni}(\text{cpsms})_2]$  reveal the presence of  $\text{Ni}\cdots\text{H}$  anagostic interactions.<sup>16</sup> The  $[\text{Ni}(\text{SS}')_2\text{Fe}(\text{C}_5\text{H}_5)(\text{CO})](\text{PF}_6)$  complexes are more efficient electrocatalysts than the  $[\text{Ni}(\text{S}_2\text{S}'_2)\text{Fe}(\text{C}_5\text{H}_5)(\text{CO})](\text{PF}_6)$  complexes based on the tetradentate ligands described in Chapter 3, most likely due to the increased flexibility of the  $\text{NiS}_4$  coordination spheres. However, two of the  $[\text{Ni}(\text{SS}')_2\text{Fe}(\text{C}_5\text{H}_5)(\text{CO})](\text{PF}_6)$  complexes are found to be less tolerant to the protic acids, since the thioether donors of these complexes are more readily protonated.<sup>19</sup> Hence, the next Chapter will be devoted to the study of a new class of  $[\text{NiRu}]$  complexes with the aim of making more stable and improved electrocatalysts.

#### 4.5. Experimental Procedures

##### 4.5.1. General Remarks

The synthesis of the ligand precursor thiouronium salts TU-cpsms, TU-mpsms, TU-ibsms, and TU-nhsms are described in Chapter 2 along with the characterizations. The mononuclear nickel complex  $[\text{Ni}(\text{bsms})_2]$  has been synthesized as reported in literature.<sup>12</sup> The complexes of general formula  $[\text{Ni}(\text{SS}')_2\text{Fe}(\text{C}_5\text{H}_5)(\text{CO})](\text{PF}_6)$  have been synthesized by slightly modifying the reported procedure.<sup>22</sup>

##### 4.5.2. Synthesis of $[\text{Ni}(\text{mpsms})_2]$

A two-necked round bottom flask was charged with  $\text{Ni}(\text{acac})_2$  (0.771 g, 3 mmol) and the thiouronium salt TU-mpsms (1.745 g, 6 mmol). To this 60 ml ethanol was added under argon atmosphere. After 10 minutes stirring at 60 °C,  $\text{NMe}_4\text{OH}$  (0.547 g, 6 mmol) was added to the green solution. After the immediate formation of a dark brown colour, the solution was refluxed for two hours, and then the reaction mixture was evaporated to dryness under reduced pressure. Dichloromethane was added to the residue and filtered through Celite until the filtrate was colourless, in order to remove the tetramethylammonium salt. The filtrate was concentrated to 1 ml before adding 100 ml hexane and the mixture was kept at 4 °C overnight. Analytically pure, dark-brown flocculent needles were collected by filtration and dried under vacuum (1.3 g, 91%).  $^1\text{H}$  NMR:  $\delta_{\text{H}}$  [399.51 MHz,  $\text{CD}_2\text{Cl}_2$ , 303 K]) 7.92 (bs, 4H, phenyl-*ortho*-H), 7.52 (d, 4H, phenyl-*meta*-H), 2.36 (s, 6H,  $\text{CH}_3$ -Ph), 2.28 (s, 4H,  $-\text{CH}_2-\text{S}-$ ), 1.28 (s, 12H,  $-\text{C}(\text{CH}_3)_2-$ ). **Elemental Analysis (%)**: calculated for  $\text{C}_{22}\text{H}_{30}\text{S}_4\text{Ni}$ , C 54.89, H 6.28, S 26.64, found,

C 55.17, H 6.66 S 24.55. **MS (ESI):** ( $m/z$ ) calculated for  $C_{22}H_{31}S_4Ni$   $[MH]^+$  requires 481.07, found 480.80.

#### 4.5.3. Synthesis of $[Ni(cpsms)_2]$

The synthesis was carried out similar to that of  $[Ni(mpsms)_2]$ . Yield: 78%.  **$^1H$  NMR:**  $\delta_H$  [399.51 MHz,  $CD_2Cl_2$ , 303 K] 8.13 (bs, 4H, phenyl-*ortho-H*), 7.25 (d, 4H, phenyl-*meta-H*), 2.42 (s, 4H,  $-CH_2-S-$ ), 1.37 (s, 12H,  $-C(CH_3)_2-$ ). **Elemental Analysis (%):** calculated for  $C_{20}H_{24}S_4NiCl_2$ , C 46.00, H 4.63, S 24.56, found, C 45.17, H 4.56 S 24.15. **MS (ESI):** ( $m/z$ ) calculated for  $C_{20}H_{25}S_4NiCl_2$   $[MH]^+$  requires 520.96, found 520.75.

#### 4.5.4. Synthesis of $[Ni(ibsms)_2]$

The synthesis was carried out similar to that of  $[Ni(mpsms)_2]$ . Yield: 63%. **Elemental Analysis (%):** calculated for  $C_{16}H_{34}S_4Ni$ , C 46.49, H 8.29, S 31.03, found, C 46.31.17, H 8.16 S 29.55. **MS (ESI):** ( $m/z$ ) calculated for  $C_{16}H_{35}S_4Ni$   $[MH]^+$  requires 413.10, found 412.93.

#### 4.5.5. Synthesis of $[Ni(nhsms)_2]$

The synthesis was carried out similar to that of  $[Ni(mpsms)_2]$ . Yield: 72%.  **$^1H$  NMR:**  $\delta_H$  [399.51 MHz,  $CD_2Cl_2$ , 303 K] 3.11 (s, 4H,  $-S-C(CH_3)_2-CH_2-S-$ ), 2.71 (t, 4H,  $CH_3-(CH_2)_4-CH_2-S-$ ), 1.91 (p, 2H,  $CH_3-(CH_2)_3-CH_2-CH_2-S-$ ), 1.58 (s, 6H,  $-S-C(CH_3)_2-CH_2-S-$ ), 1.39 (m, 6H,  $CH_3-(CH_2)_3-(CH_2)_2-S-$ ), 0.89 (t, 6H,  $CH_3-$ ). **Elemental Analysis (%):** calculated for  $C_{20}H_{42}S_4Ni$ , C 51.16, H 9.02, S 27.32, found, C 52.17, H 9.36 S 26.55. **MS (ESI):** ( $m/z$ ) calculated for  $C_{20}H_{43}S_4Ni$   $[MH]^+$  requires 469.16, found 468.98.

#### 4.5.6. Synthesis of $[Ni(bsms)_2Fe(C_5H_5)CO](PF_6)$

The synthesis was carried out by modifying the procedure described in the literature.<sup>22</sup> Yield 27%. **Elemental analysis:** Calcd (%) for  $C_{28}H_{35}OS_4NiFePF_6$ , 775.35: C 43.37, H 4.55, S 16.54, found: C 42.91 H 4.23 S 16.18. **MS (ESI):** ( $m/z$ ) calculated for  $C_{28}H_{35}S_4ONiFe$   $[M-PF_6]$  requires (monoisotopic mass) 629.03, found 628.72; calculated for  $C_{27}H_{35}S_4NiFe$   $[M-(CO+PF_6)]$  requires 601.03, found 600.80; calculated for  $C_{22}H_{30}S_4NiFe$   $[M-(C_5H_5+CO+PF_6)]$  requires 535.99, found 535.70.

#### 4.5.7. Synthesis of $[Ni(mpsms)_2Fe(C_5H_5)CO](PF_6)$

The synthesis was carried out by modifying the procedure described in the literature.<sup>22</sup> Yield 24%. **Elemental analysis:** Calcd (%) for  $C_{28}H_{35}OS_4NiFePF_6$ , 775.35: C 43.37, H 4.55, S 16.54, found: C 43.11 H 4.28 S 16.31. **MS (ESI):** ( $m/z$ ) calculated for  $C_{28}H_{35}S_4ONiFe$   $[M-PF_6]$  requires (monoisotopic mass) 629.03, found 628.76; calculated for  $C_{27}H_{35}S_4NiFe$   $[M-(CO+PF_6)]$  requires 601.03, found 600.58; calculated for  $C_{22}H_{30}S_4NiFe$   $[M-(C_5H_5+CO+PF_6)]$  requires 535.99, found 535.73

#### 4.5.8. Synthesis of [Ni(cpsms)<sub>2</sub>Fe(C<sub>5</sub>H<sub>5</sub>)CO](PF<sub>6</sub>)

The synthesis was carried out by modifying the procedure described in the literature.<sup>22</sup> Yield 19%. **Elemental analysis:** Calcd (%) for C<sub>26</sub>H<sub>29</sub>OS<sub>4</sub>NiCl<sub>2</sub>FePF<sub>6</sub>, 816.19: C 38.26, H 3.58, S 15.72, found: C 37.85 H 3.23 S 15.48. **MS (ESI):** (*m/z*) calculated for C<sub>22</sub>H<sub>29</sub>S<sub>4</sub>ONiCl<sub>2</sub>Fe [M-PF<sub>6</sub>] requires (monoisotopic mass) 668.92, found 668.60; calculated for C<sub>22</sub>H<sub>29</sub>S<sub>4</sub>NiCl<sub>2</sub>Fe [M-(CO+PF<sub>6</sub>)] requires 604.92, found 604.62.

#### 4.5.9. Synthesis of [Ni(ibsms)<sub>2</sub>Fe(C<sub>5</sub>H<sub>5</sub>)CO](PF<sub>6</sub>)

The synthesis was carried out by modifying the procedure described in the literature.<sup>22</sup> Yield 17%. **Elemental analysis:** Calcd (%) for C<sub>22</sub>H<sub>39</sub>OS<sub>4</sub>NiFePF<sub>6</sub>, 707.32: C 37.36, H 5.56, S 18.13, found: C 37.25 H 5.33 S 17.99. **MS (ESI):** (*m/z*) calculated for C<sub>22</sub>H<sub>39</sub>S<sub>4</sub>ONiFe [M-PF<sub>6</sub>] requires (monoisotopic mass) 561.06, found 560.79; calculated for C<sub>21</sub>H<sub>39</sub>S<sub>4</sub>NiFe [M-(CO+PF<sub>6</sub>)] requires 533.06, found 532.90.

#### 4.5.10. Synthesis of [Ni(nhsms)<sub>2</sub>Fe(C<sub>5</sub>H<sub>5</sub>)CO](PF<sub>6</sub>)

The synthesis was carried out by modifying the procedure described in the literature.<sup>22</sup> Yield 21%. **Elemental analysis:** Calcd (%) for C<sub>26</sub>H<sub>47</sub>OS<sub>4</sub>NiFePF<sub>6</sub>, 763.43: C 40.91, H 6.21, S 16.80, found: C 41.0745 H 6.33 S 16.58. **MS (ESI):** (*m/z*) calculated for C<sub>26</sub>H<sub>47</sub>S<sub>4</sub>ONiFe [M-PF<sub>6</sub>] requires (monoisotopic mass) 617.12, found 616.94; calculated for C<sub>25</sub>H<sub>47</sub>S<sub>4</sub>NiFe [M-(CO+PF<sub>6</sub>)] requires 589.13, found 588.87.

#### 4.5.11. Crystallographic Data of Complex [Ni<sub>3</sub>(cpsms)<sub>6</sub>]

C<sub>60</sub>H<sub>72</sub>Cl<sub>6</sub>Ni<sub>3</sub>S<sub>12</sub>·CH<sub>2</sub>Cl<sub>2</sub>, Fw = 1651.65, brown plates, 0.06 × 0.14 × 0.34 mm<sup>3</sup>, monoclinic, *C2c* (no. 15), *a* = 52.445(2), *b* = 11.5078(7), *c* = 27.6319(10) Å, α = 90, β = 116.548(2), γ = 90°, *V* = 14918.2(12) Å<sup>3</sup>, *Z* = 8, *D<sub>x</sub>* = 1.471 g cm<sup>-3</sup>, μ = 1.409 mm<sup>-1</sup>. 102595 Reflections were measured up to a resolution of (sin θ/λ)<sub>max</sub> = 0.65 Å<sup>-1</sup>. An absorption correction based on multiple measured reflections was applied (0.33–0.86 correction range). 14648 Reflections were unique (*R*<sub>int</sub> = 0.061), of which 10522 were observed [*I* > 2σ(*I*)]. 797 Parameters were refined with no restraints. *R1/wR2* [*I* > 2σ(*I*)]: 0.0203/0.0387. *R1/wR2* [all refl.]: 0.0496/0.0890. *S* = 1.04. Residual electron density was found between -0.84 and 1.25 eÅ<sup>-3</sup>.

## 4.6. References

1. J. A. W. Verhagen, PhD Thesis, *Structural Models of Nickel-Containing Enzymes*, Leiden University, 2004.
2. J. R. Nicholson, G. Christou, J. C. Huffman and K. Folting, *Polyhedron*, 1987, **6**, 863-870.
3. N. Baidya, P. K. Mascharak, D. W. Stephan and C. F. Campagna, *Inorg. Chim. Acta*, 1990, **177**, 233-238.
4. T. Yamamura, H. Kurihara, N. Nakamura, R. Kuroda and K. Asakura, *Chem. Lett.*, 1990, 101-104.



## Chapter 4

5. B. S. Snyder, C. P. Rao and R. H. Holm, *Aust. J. Chem.*, 1986, **39**, 963-974.
6. D. Sellmann, S. Funfgelder, F. Knoch and M. Moll, *Z.Naturforsch.(B)*, 1991, **46**, 1601-1608.
7. M. Y. Cha, C. L. Catlin, S. C. Critchlow and J. A. Kovacs, *Inorg. Chem.*, 1993, **32**, 5868-5877.
8. M. Cha, J. Sletten, S. Critchlow and J. A. Kovacs, *Inorg. Chim. Acta*, 1997, **263**, 153-159.
9. T. Yamamura, H. Arai, H. Kurihara and R. Kuroda, *Chem. Lett.*, 1990, 1975-1978.
10. E. Erkizia and R. R. Conry, *Inorg. Chem.*, 2000, **39**, 1674-1679.
11. S. Fox, Y. Wang, A. Silver and M. Millar, *J. Am. Chem. Soc.*, 1990, **112**, 3218-3220.
12. J. A. W. Verhagen, D. D. Ellis, M. Lutz, A. L. Spek and E. Bouwman, *J. Chem. Soc.-Dalton Trans.*, 2002, 1275-1280.
13. J. A. W. Verhagen, M. Beretta, A. L. Spek and E. Bouwman, *Inorg. Chim. Acta*, 2004, **357**, 2687-2693.
14. J. A. W. Verhagen, C. Tock, M. Lutz, A. L. Spek and E. Bouwman, *Eur. J. Inorg. Chem.*, 2006, 4800-4808.
15. J. S. Kim, J. H. Reibenspies and M. Y. Darensbourg, *J. Am. Chem. Soc.*, 1996, **118**, 4115-4123.
16. R. Angamuthu, L. L. Gelauff, M. A. Siegler, A. L. Spek and E. Bouwman, *Chem. Commun.*, 2009, 2700-2702.
17. F. Lauderbach, R. Prakash, A. W. Götz, M. Munoz, F. W. Heinemann, U. Nickel, B. A. Hess and D. Sellmann, *Eur. J. Inorg. Chem.*, 2007, 3385-3393.
18. S. Ott, M. Kritikos, B. Åkermark, L. C. Sun and R. Lomoth, *Angew. Chem.-Int. Edit.*, 2004, **43**, 1006-1009.
19. R. Angamuthu and E. Bouwman, *Phys. Chem. Chem. Phys.*, 2009, **11**, 5578-5583.
20. B. Keita, S. Floquet, J. F. Lemonnier, E. Cadot, A. Kachmar, M. Benard, M. M. Rohmer and L. Nadjò, *J. Phys. Chem. C*, 2008, **112**, 1109-1114.
21. R. Angamuthu, H. Kooijman, M. Lutz, A. L. Spek and E. Bouwman, *Dalton Trans.*, 2007, 4641-4643.
22. W. F. Zhu, A. C. Marr, Q. Wang, F. Neese, D. J. E. Spencer, A. J. Blake, P. A. Cooke, C. Wilson and M. Schröder, *Proc. Natl. Acad. Sci. U. S. A.*, 2005, **102**, 18280-18285.